

Article

Influence of Si Substrate Preparation Procedure on Polarity of Self-Assembled GaN Nanowires on Si(111): Kelvin Probe Force Microscopy Studies

Marta Sobanska ^{1,*} , Núria Garro ², Kamil Klosek ¹, Ana Cros ² and Zbigniew R. Zytkeiwicz ¹ 

¹ Institute of Physics of Polish Academy of Sciences, Al. Lotnikow 32/46, 02-668 Warsaw, Poland; klosek@ifpan.edu.pl (K.K.); zytke@ifpan.edu.pl (Z.R.Z.)

² Institute of Materials Science, University of Valencia, E-46071 Valencia, Spain; nuria.garro@uv.es (N.G.); ana.cros@uv.es (A.C.)

* Correspondence: sobanska@ifpan.edu.pl

Received: 26 October 2020; Accepted: 11 November 2020; Published: 13 November 2020



Abstract: The growth of GaN nanowires having a polar, wurtzite structure on nonpolar Si substrates raises the issue of GaN nanowire polarity. Depending on the growth procedure, coexistence of nanowires with different polarities inside one ensemble has been reported. Since polarity affects the optical and electronic properties of nanowires, reliable methods for its control are needed. In this work, we use Kelvin probe force microscopy to assess the polarity of GaN nanowires grown by plasma-assisted Molecular Beam Epitaxy on Si(111) substrates. We show that uniformity of the polarity of GaN nanowires critically depends on substrate processing prior to the growth. Nearly 18% of nanowires with reversed polarity (i.e., Ga-polar) were found on the HF-etched substrates with hydrogen surface passivation. Alternative Si substrate treatment steps (RCA etching, Ga-triggered deoxidation) were tested. However, the best results, i.e., purely N-polar ensemble of nanowires, were obtained on Si wafers thermally deoxidized in the growth chamber at ~1000 °C. Interestingly, no mixed polarity was found for GaN nanowires grown under similar conditions on Si(111) substrates with a thin AlO_y buffer layer. Our results show that reversal of nanowires' polarity can be prevented by growing them on a chemically uniform substrate surface, in our case on clean, in situ formed SiN_x or ex situ deposited AlO_y buffers.

Keywords: gallium nitride nanowires; polarity; Kelvin probe force microscopy

1. Introduction

GaN nanowires (NWs) are found as promising building blocks for a future generation of electronic and optoelectronics devices. In general, NWs are almost strain-free objects without lattice misfit defects propagating into the crystalline structure even if grown on highly lattice-mismatched substrates. Therefore, these nanostructures facilitate, for instance, the integration of GaN-based devices with Si electronics. In addition, complicated heterostructures can be ideally grown in the form of NWs with a crystallographic quality not achievable in the case of comparable planar heterostructures. However, the growth of wurtzite GaN nanowires on nonpolar Si substrates raises the issue of GaN NW polarity, which is known to have a critical impact on the structural properties of GaN, such as the incorporation of dopants [1–4], surface reactivity [5] and thermal stability [6], as well as on the nucleation and growth of GaN NWs [7,8]. Polarity also causes the onset of a spontaneous built-in electric field in nitride heterostructures, which, together with a piezoelectric contribution due to strain-related electric polarization, accounts for polarization-induced doping [9] and the formation of two-dimensional electron gas in high-electron mobility transistor structures [10]. Overall, polarity significantly affects

the performance of GaN-based devices, so it must be carefully controlled and kept uniform over a large surface area.

While in planar films one polarization domain may overgrow the other and result in a single film polarity [11], this is very unlikely in NWs due to their low lateral growth rate. It is well established already that GaN NWs grow exclusively under N-rich conditions with the *c*-axis parallel to the growth direction [12–18]. There is no consensus, however, about NW polarity. Although the majority of self-assembled GaN NWs grown on Si substrates are found to be N-polar, the coexistence of NWs with different polarities inside the NW ensemble has been observed [9,11,19–22]. The formation of mixed-polarity NWs is not fully understood and the parameters influencing this behavior, which include the interface chemistry and the growth procedure, are still under debate. However, it is widely reported that the polarity of self-assembled NWs is determined at the GaN nucleation stage and can be reversed from N- to Ga-polar by the high local surface concentration of impurities like Mg, Si, Ti or O [20,23–30]. These findings clearly indicate that proper substrate preparation is decisive for the achievement of homogeneous polarity. In particular, in the case of growth on Si surfaces, the processing procedure and cleanness of Si further determine the chemical and morphological uniformity of the silicon nitride film created during a Si nitridation step prior to GaN growth. As will be shown, these are critical steps for the successful formation of GaN NW ensembles with uniform N polarity.

In this work, we tested the procedures commonly used to prepare Si(111) substrates prior to plasma-assisted molecular beam epitaxial (PAMBE) growth of GaN NWs regarding their impact on the polarity of ensembles of self-assembled GaN nanowires. From a wide range of techniques used to determine the polarity of NWs (see [31] for a review), Kelvin probe force microscopy (KPFM) was chosen. By contrast to the techniques based on electron microscopy which require complicated sample preparation, are time-demanding and may lead to sample damage, KPFM allows the polarity assessment of a statistically significant number of single NWs over micrometer large surface areas with nanometer resolution and without the need of any special sample preparation [32]. Our studies show that the uniformity of the polarity of GaN NWs on Si(111) strongly depends on the procedure used for the substrate processing prior to NW growth. Interestingly, no mixed polarity was found for GaN NWs grown under similar conditions on Si(111) substrates covered by a thin amorphous AlO_y buffer layer [33,34]. This shows the crucial role the chemistry at the GaN/Si(111) interface plays for the determination of GaN NWs polarity.

2. Experiment

The samples used in this study were grown by PAMBE using a solid-source effusion Ga cell and the radio frequency Addon nitrogen plasma source controlled by an optical sensor of plasma light emission [35]. All samples were grown on n-type low-resistivity (1–30 Ωcm) silicon (111) substrates. Five of them, later referred to as samples A–E, were grown on bare silicon and they differ only by the procedure used for Si substrate cleaning before epitaxial growth. Details of these procedures are listed in Table 1. Irrespective of substrate preparation, all wafers were transferred in air to the PAMBE system and outgassed in the loading chamber at ~150 °C for 1 h and then at ~400 °C in the preparation chamber for 2 h to remove any volatile contamination before the transfer to the growth chamber. The substrate temperature was calibrated prior to growth on bare Si(111) substrate by observation of the 7 × 7 to 1 × 1 reflection high-energy electron diffraction (RHEED) pattern transition at 830 °C [36,37]. The growth procedure started by exposing silicon substrates to an active nitrogen flux for 15 min at 750 °C. The aim was to create a thin SiN_x film on the surface as explained in detail in our previous report [17]. Finally, the Ga source was opened to induce incubation of three-dimensional GaN islands which subsequently transformed to NWs [38–41]. In addition, sample F was grown on Si(111) deoxidized by the HF dip, similar to sample A, and then transferred in air to the atomic layer deposition (ALD) system for the deposition of a 15 nm thick amorphous AlO_y buffer layer at 85 °C [42]. Then, the substrate was loaded to the PAMBE system, degassed in loading and preparation chambers as for the rest of the samples and transferred to the growth chamber. No substrate nitridation was used for that sample and, after

reaching the growth temperature and ignition of the N source, the Ga and N shutters were opened simultaneously to start the growth. All samples reported in this work were grown at the temperature of 750 °C and under nitrogen-rich conditions (N/Ga flux ratio of 1.8) to promote NW growth.

Table 1. Substrate preparation steps used for samples A–F. The last column shows the number of nanowires (NWs) analyzed by KPFM and the percentage of NWs with a polarity flip from N to Ga.

Sample	Description of Si Substrate Processing Procedure	% of Ga-Polar NWs
A	Aqueous HF dip followed by thermal desorption of hydrogen passivation in the growth chamber at ~700 °C	18% Ga-polar (125 NWs tested)
B	RCA clean followed by thermal removal of silicon oxide in the growth chamber at ~950 °C for 10 min	4% Ga polar (50 NWs tested)
C	Procedure as for sample B followed by 2 × Ga-induced deoxidation steps in the growth chamber	<3% Ga-polar (180 NWs tested)
D	Thermal oxide desorption in UHV at ~1000 °C for 10 min followed by 2 × Ga-induced deoxidation steps as for sample C	0% Ga-polar (225 NWs tested)
E	Thermal native oxide desorption in the growth chamber at ~1000 °C for 10 min	0% Ga-polar (120 NWs tested)
F	Aqueous HF dip as for sample A followed by transfer in air to the ALD system for deposition of AlO _y buffer	0% Ga-polar (>400 NWs tested)

Frequency-modulation KPFM was used to nondestructively determine the polarity of individual NWs within the assembly. The technique is based on the local measurement of the contact potential difference (CPD) between the NW top facet and the atomic force microscopy (AFM) tip [43,44]. Assuming similar electron affinities in N- and Ga-polar GaN, the measured CPD is used to reveal differences in the work function between polar faces [31], which allows their identification [45]. Calibration of the tip contact potential was performed by measuring the CPD on the N- and the Ga-polar facets of a GaN bulk sample grown by hydride vapor-phase epitaxy. For all Pt-coated tips used, the resulting CPD was typically comprised in the interval of 0.20–0.35 V for the Ga-polar face and 0.75–0.90 V for the N-polar face, the difference between N- and Ga-polar faces measured with the same tip being constant (0.55 ± 0.05 V). Complementary images of KPFM, namely topography and contact potential difference, were analyzed [32]. They allow measuring the polarity of individual NWs over an area of tens of μm^2 and provide good statistics on the polarity of the ensemble.

3. Results and Discussion

Figure 1a shows the AFM topographic view image of sample A. The NWs have a diameter of ~200 nm, but this is convoluted with the tip, which has a diameter of ~20 nm. Figure 1b shows a CPD map of the same area. Some darker NWs, marked by blue arrows, are clearly visible on the map. Figure 1c,d present the CPD value and NW height profiles along the green line, respectively. As seen in Figure 1b,c, the mean CPD value for the majority of the NWs is ~1000 mV, which is compatible with their N polarity. On the contrary, for dark NWs marked by blue arrows, the CPD values drop to ~350 mV. Those values could be attributed to a reverse polarity in Ga-polar NWs. As shown in the last column of Table 1, nearly 18% of 125 NWs checked in total in sample A exhibited reversed polarity.

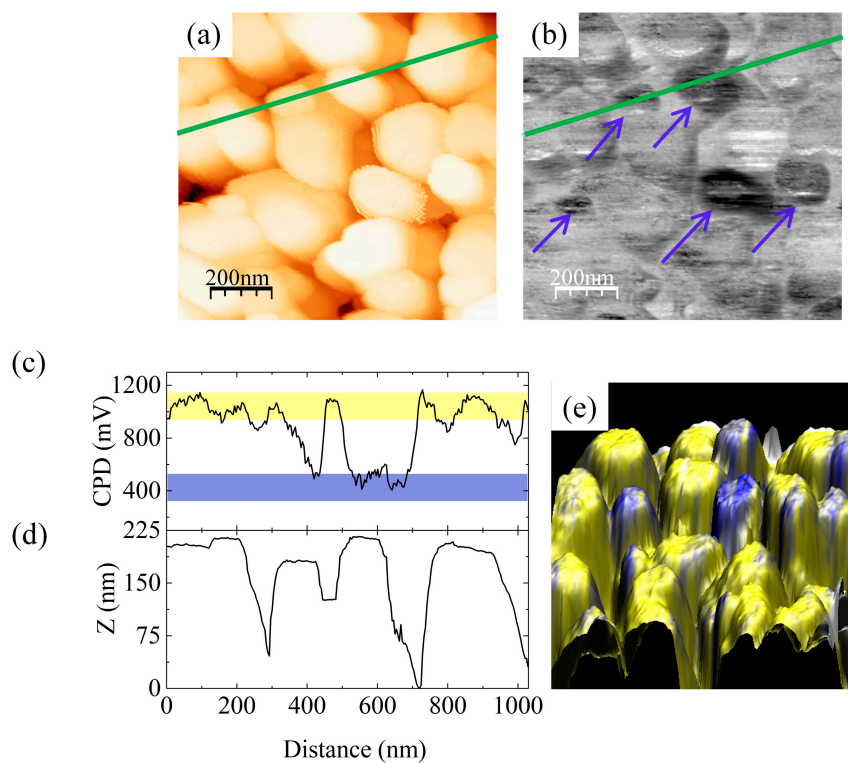


Figure 1. (a) AFM topographic view image ($1 \times 1 \mu\text{m}^2$, color scale from 0 to 370 nm) and (b) the corresponding contact potential difference (CPD) map (color scale from 0 to 1.5 V) of sample A. Blue arrows in (b) mark Ga-polar NWs. The CPD value and NW height profiles along the green line, (c) and (d), respectively. (e) shows the 3D superposition of the topography (xyz axis) and CPD value (color scale). Blue marks Ga-polar and yellow N-polar NWs.

Dipping of the as-received wafer in diluted ($\sim 5\%$) HF acid is the most commonly used procedure for Si substrate preparation before GaN NWs growth by PAMBE [46–50]. This is due to the simplicity of the technique. Moreover, the high-temperature substrate heater required by other methods is not needed. There are a number of studies showing that etching of silicon in a solution of HF removes native silicon oxide and results in hydrogen-terminated and locally ordered surfaces. [51–54]. The hydrogen surface passivation provides protection against oxygen during the wafer transfer to the ultra-high vacuum (UHV) system, where it is removed by annealing at moderate temperatures. Unfortunately, it degrades with exposure to air and moisture. Therefore, the efficiency of surface protection critically depends on the handling of the etched sample. In particular, the time of surface exposure to the laboratory air before transfer to the UHV chamber must be made as short as possible. Moreover, the use of a glove box with dry inert atmosphere connected to the load lock chamber to prevent exposure of the freshly etched sample to oxygen is recommended [55].

Mixed polarity of GaN NWs grown by PAMBE on HF-treated Si substrates is widely observed. Concordel et al. reported the amount of Ga-polar NWs to be below a small percent [20], while the KPFM studies by Minj et al. revealed $\sim 5\%$ of GaN NWs with Ga instead of N polarity [32]. Although these values are much lower than those found in our study, direct comparison is not straight forward since most publications do not provide a precise description of how the freshly etched substrates have been handled.

In the case of sample A, prior to the NW growth, the Si(111) substrate was etched in 5% aqueous HF solution for 1 min, followed by a short deionized water bath and drying with nitrogen. Then, it was transferred in air to the MBE system. The freshly etched substrate was exposed to the air for ~ 10 min until pumping of the load lock chamber started. After initial thermal treatment in the load chamber as described in Section 2 above, the hydrogen passivation was removed by substrate

annealing in the growth chamber at a temperature of ~ 700 °C. This resulted in a sharp 7×7 RHEED pattern characteristic of a clean, oxide-free Si(111) surface. Despite that, presumably some oxide islands were left on the surface. As proposed by Borysiuk et al. [19], these islands might locally protect the Si(001) substrate against the creation of a SiN_x amorphous layer during the substrate exposure to the nitrogen flux. Thus, after the nitridation stage, the surface was covered by a silicon nitride amorphous layer with some spots of silicon oxide where GaN nucleated, first as zinc-blende (ZB) GaN pyramids and then transformed into wurzite Ga-polar GaN NWs [19].

The hypothesis that on the HF-treated Si substrate the islands of residual oxide were responsible for inducing Ga-polar growth of GaN NWs is strongly supported by results of recent X-ray diffraction measurements [56]. Due to the high intensity of the synchrotron radiation beam used and the application of grazing incidence geometry, the presence of tiny ZB-GaN pyramids that are the seeds for Ga-polar NWs could be detected on the HF-treated Si(001) substrate. For that study, we used a GaN NWs sample grown on HF-treated Si(001). We then compared the results with those obtained for NWs grown on a similar substrate, but for which, after H passivation desorption and substrate nitridation, the so-called gallium-induced surface cleaning [57–60] was used. The procedure consisted of the deposition of a few monolayers of Ga at a low temperature of 500 °C in the absence of active nitrogen, followed by gallium desorption at 800 °C. This step was repeated three times, after which the substrate was nitridated again. It is well established that Ga-induced cleaning leads to the creation of volatile Ga_2O on the substrate that is removed from the surface during heating [61,62]. We anticipated that if after the first nitridation step the substrate was cleaned by gallium flux, the residual silicon oxide islands should be removed, so the second nitridation step could complete the SiN_x film on places initially covered by the oxide. As a result, the concentration of ZB-GaN pyramids should be significantly reduced. This was indeed observed, together with a corresponding reduction in the number of Ga-polar NWs [56].

In silicon manufacturing, the standard way of treating Si wafers before high-temperature processing steps is the well-known RCA clean developed by the Radio Corporation of America in 1965 [63]. In this cleaning procedure, the native oxide on silicon is dissolved and a new oxide layer forms. Such oxide regeneration is an important factor in the removal of particles and chemical impurities from the surface. The thin volatile oxide created on the wafer may be removed at ~ 800 °C under UHV if a pure silicon surface is needed for epitaxial growth [13,38,64–67]. The Si substrate for sample B was prepared by its exposure for 10 min to a mixture of water-diluted hydrogen peroxide and ammonium hydroxide at 80 °C (SC-1 bath), followed by a short immersion in a 1:20 solution of aqueous HF (oxide removal) and a final etching in a mixture of water-diluted hydrogen peroxide and hydrochloric acid at 80 °C for 10 min (SC-2 bath) [68]. After the deionized water rinse and drying in nitrogen flow, the substrate was annealed in the PAMBE growth chamber at ~ 950 °C for 10 min to desorb the oxide film. Next, standard substrate nitridation and GaN NW growth were performed. KPFM studies of the as-prepared sample B revealed that 4% of the 50 NWs checked exhibited reversed polarity. This result is similar to that reported by Eftychis et al., who used KOH etching to assess the polarity of GaN NWs grown by PAMBE on RCA-cleaned Si(111) substrates [65].

Interestingly, if after desorption of the oxide film formed by the RCA clean two Ga-triggered deoxidation steps were additionally applied (sample C), the number of Ga-polar NWs reduced only slightly to $\sim 3\%$ (180 NWs analyzed in total). This indicates that oxides were only a fraction of the impurities responsible for the reversed polarity, while the majority of them most probably originated from a residual contamination of chemicals, water, glassware or handling tools.

Next, sample D was prepared, for which, instead of using the RCA clean, the native oxide was thermally desorbed from an as-received wafer in the PAMBE growth chamber at ~ 1000 °C for 10 min. Then, two Ga-induced surface deoxidation steps were applied before substrate nitridation as for sample C. KPFM studies showed that none of the 225 NWs tested in sample D exhibited Ga polarity. In order to elucidate whether this was due to the thermal oxide desorption itself or the Ga-triggered

deoxidation, sample E was studied for which the substrate was prepared as for sample D but without the Ga-induced surface cleaning steps.

Figure 2a,b show, respectively, the AFM topographic view image and the CPD map of the same area of sample E. The profile in Figure 2c shows a uniform CPD distribution with the mean value of ~ 850 mV, which is compatible with the nitrogen polarity of the NWs. No dark spots corresponding to Ga-polar NWs, as those marked with arrows in Figure 1b, are found on the CPD map of sample E (120 NWs analyzed in total). This evidences that thermal native oxide desorption at high temperature alone provides a clean Si surface and that additional Ga-triggered deoxidation steps, as those used for sample D, are not necessary. However, it is worthy noticing that results of the substrate cleaning procedure may depend on the particular conditions available in various laboratories. For instance, Carnevalle et al. reported $\sim 10\%$ of Ga-polar NWs grown by PAMBE on Si(111) substrates thermally deoxidized in the growth chamber at a temperature of ~ 1000 °C [9], i.e., under conditions similar to those used for sample E.

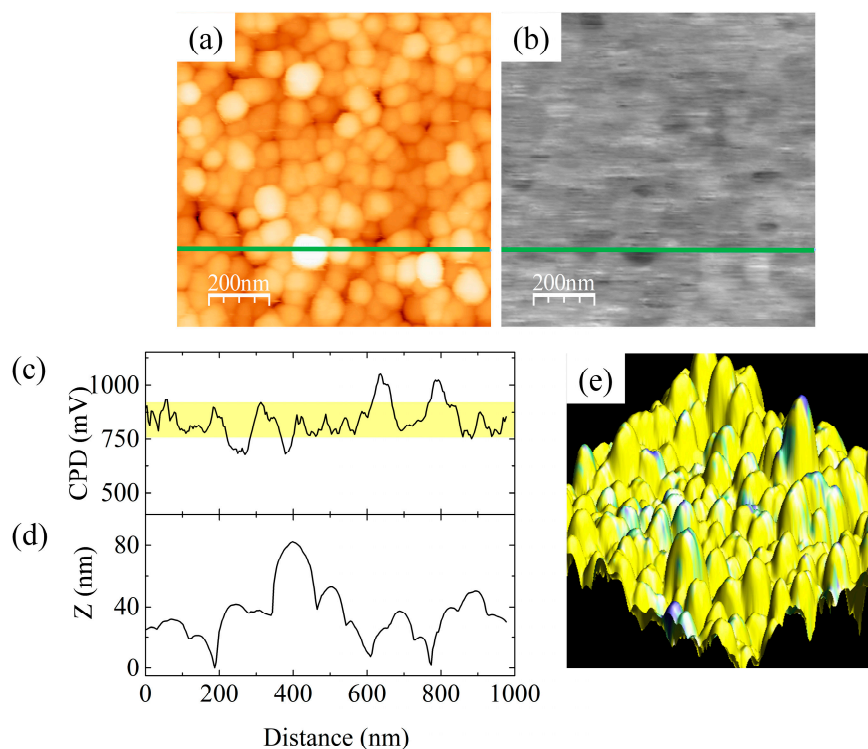


Figure 2. (a) AFM topographic view image ($1 \times 1 \mu\text{m}^2$, color scale from 0 to 100 nm) and (b) the corresponding CPD map (color scale from 0 to 1.5 V) of sample E. The CPD value and NW height profiles along the green line, (c) and (d), respectively. (e) shows the 3D superposition of the topography (xyz axis) and CPD value (color scale).

In summary, from the silicon substrate cleaning procedures tested in this work, thermal native oxide desorption at high temperature inside the growth chamber provides the best uniformity of polarity in the GaN NWs ensemble. Obviously, the cleaner the surface of the silicon substrate before its nitridation, the cleaner and more chemically uniform the silicon nitride layer on which NWs nucleate. If any contamination is left on the Si surface, it disturbs the SiN_x nucleation layer and may lead to the formation of NWs with reversed polarity. We underline that each of the substrate cleaning techniques presented above resulted in a sharp 7×7 RHEED pattern characteristic of a clean, oxide-free Si(111) surface prior to the switching on the nitrogen source. Results of our KPFM studies show that this is not sufficient to ensure uniform N polarity in the whole NW ensemble.

Another strategy for the formation of polarity-uniform GaN NWs arrays by PAMBE is to grow them on a thin uniform buffer layer deposited ex situ on the silicon substrate. If such a buffer is

chemically stable and conformally buries residual impurities on the substrate, it should prevent NW polarity reversal from N to Ga.

Recently, there is an increasing interest in the application of amorphous AlO_y films deposited by ALD as nucleation layers for the PAMBE growth of GaN nanostructures. Such buffers effectively induce selective area formation of GaN NWs on sapphire [33] and GaN [69,70]. As shown in previous studies [34,41,71,72], AlO_y buffer layers significantly enhance the nucleation rate of GaN with respect to nitridated Si without a loss of structural and optical quality [34]. Additionally, AlO_y buffers prevent diffusion of silicon from the substrate [34], facilitating the growth of GaN nanostructures at high temperatures without incorporating any impurities [73], thus potentially leading to exceptional optical properties. However, the polarity of GaN NWs grown by PAMBE on Si(111) substrate with a thin AlO_y buffer layer deposited by ALD has never been tested. In this study, we used KPFM to fill this gap.

Figure 3a shows the AFM topographic view image of sample F. The NWs have a diameter of ~ 90 nm, but as before, this is convoluted with the AFM tip of ~ 20 nm diameter. The CPD values shown in the map in Figure 3b and in the CPD line profile in Figure 3c are quite uniform with the mean value of ~ 750 mV, which is compatible with the N polarity of the NWs. In some points of the map, the CPD value slightly decreases to ~ 450 mV, but these points do not correspond to the top of the NWs and are assigned to NWs' sidewalls. This allows us to conclude that no mixed polarity with a certainty above 99.8% (more than 400 NWs analyzed) was observed for GaN NWs grown on Si(111) substrates covered by a thin amorphous AlO_y buffer layer.

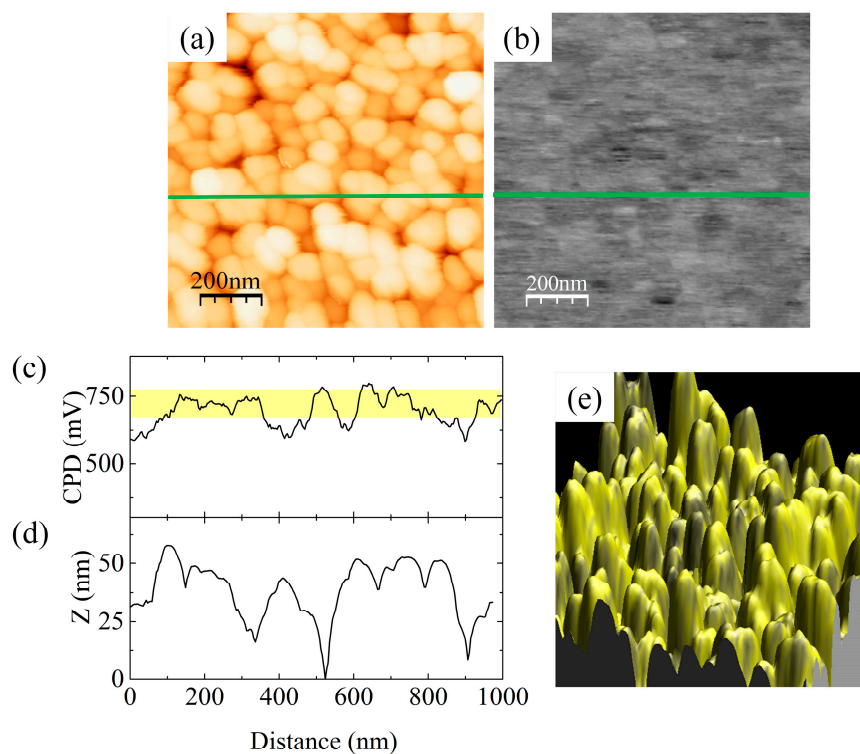


Figure 3. (a) AFM topographic view image ($1 \times 1 \mu\text{m}^2$, color scale from 0 to 140 nm) and (b) the corresponding CPD map (color scale from 0 to 1.5 V) of sample F. The CPD value and NW height profiles along the green line, (c) and (d), respectively. (e) shows the 3D superposition of the topography (xyz axis) and CPD value (color scale).

Finally, it is worth mentioning that the silicon substrate for sample F was cleaned by a HF dip in the same procedure as used for sample A, and then transferred in air to the ALD system. It took a few hours before the deposition of the buffer layer started. Due to the instability of the H-passivated substrate surface, it certainly got locally oxidized during the long time of unprotected storage. Nevertheless, no

reversed NW polarity was found in sample F. This indicates that the islands of oxide that led to the appearance of Ga-polar NWs in sample A were efficiently covered by the buffer and their presence under the amorphous AlO_y layer had no impact on GaN nucleation.

4. Summary and Conclusions

In this work, the most common procedures used to process Si substrates prior to epitaxial growth are tested to find their impact on polarity uniformity inside the ensemble of self-assembled GaN NWs grown by PAMBE. Since local contamination of the silicon substrate surface eventually disturbs the uniformity of the SiN_x film formed during the nitridation step preceding the GaN nucleation, this might lead to the formation of NWs with reversed Ga polarity.

Kelvin probe force microscopy was used to determine the polarity of GaN NWs. The technique allows the polarity assessment of a statistically significant number of single NWs on the wafer over micrometer large surface areas with nanometer resolution and without the need of any special sample preparation. Complementary images of KPFM, namely topography and contact potential difference, were analyzed.

We showed that the uniformity of the polarity within the ensemble of GaN NWs on Si(111) strongly depends on the procedure used for substrate cleaning. As high as 18% of NWs with reversed polarity (i.e., Ga-polar) were detected by KPFM if the Si substrate was etched in diluted HF and then annealed in the growth chamber to remove hydrogen passivation prior to the substrate nitridation. We ascribe this behavior to the low stability of the hydrogen passivation layer. Apparently, it did not sufficiently protect the freshly etched substrate during its transfer to the UHV system and some islands of oxide were formed, which induced the growth of Ga-polar GaN NWs by the mechanism reported earlier [19]. Such conclusion is strongly supported by previous studies showing that the mixed polarity of GaN NWs on HF-treated Si can be eliminated by additional Ga-triggered deoxidation of the substrate performed just before its nitridation inside the growth chamber [56].

Much better homogeneity of NW polarity was obtained on the Si substrate cleaned by the RCA procedure in which the native oxide was dissolved and a new oxide layer was formed. Next, this oxide was desorbed by annealing in the PAMBE growth chamber at ~ 950 °C for 10 min. KPFM studies of an NW ensemble grown on such substrate revealed that around 4% of NWs had reversed polarity. This number decreased to less than 3% if after oxide desorption, but before the nitridation step, the substrate was additionally cleaned by Ga-triggered deoxidation. In the latter case, the polarity flip could be due to surface contamination by residual pollution of chemicals, water, glassware or handling tools, instead of local surface oxidation.

The best results, i.e., purely N-polar ensemble of NWs, were obtained on epi-ready Si wafers thermally deoxidized in the growth chamber at ~ 1000 °C just prior to their nitridation. Additional Ga-induced surface cleaning steps were not needed in that case. Our studies indicate that high-temperature silicon oxide desorption under UHV produces the cleanest Si surface, resulting in the formation of a uniform SiN_x layer that prevents an NW polarity reversal from N to Ga. This requires, however, that a high-temperature substrate heater is available in the PAMBE system, which is not always the case.

It is worth mentioning that each substrate cleaning technique tested in this work resulted in a sharp 7×7 RHEED pattern characteristic of a clean Si(111) surface prior to switching the nitrogen source on. Results of our KPFM studies show that this is not sufficient to ensure uniform N polarity in the whole NW ensemble.

Finally, no mixed polarity with a certainty above 99.8% was found for GaN NWs grown under similar conditions on Si(111) substrates covered by a thin amorphous AlO_y buffer layer. It is well known that the ALD technique produces compact, pinhole-free layers conformally covering the surface. Our results indicate that an ALD-deposited AlO_y buffer efficiently buries oxides that might eventually form during a few hours' storage in air of the HF-dipped Si wafer before buffer deposition in the ALD system. Therefore, possible contamination of the substrate surface under the amorphous AlO_y layer

had no impact on GaN polarity. In summary, our results show that reversal of GaN nanowires' polarity can be efficiently prevented by growing them on a chemically uniform substrate surface, in our case on clean, in situ formed SiN_x or ex situ deposited AlO_y buffers.

Author Contributions: Conceptualization, M.S., N.G., K.K., A.C., and Z.R.Z.; methodology, M.S., N.G., A.C., and Z.R.Z.; software, N.G. and A.C.; investigation, M.S., N.G., and A.C.; resources, M.S. and K.K.; writing—original draft preparation, M.S. and Z.R.Z.; writing—review and editing, M.S., N.G., A.C., K.K., and Z.R.Z.; supervision, A.C. and Z.R.Z.; funding acquisition, A.C., N.G., and Z.R.Z. All authors have read and agreed to the published version of the manuscript.

Funding: M.S. and Z.R.Z. acknowledge partial support from the Polish National Science Centre grant 2016/23/B/ST7/03745 and the Polish National Centre for Research and Development project PBS1/A3/1/2012 Pol-HEMT. N.G. and A.C. are grateful for support from the Generalitat Valenciana (Spain), grant PROMETEO2018/123 EFIMAT and PID2019-104272RB-C53, co-financed by the Spanish MICINN and FEDER funds.

Acknowledgments: The authors thank S. Gieraltowska for ALD deposition of AlO_y buffer layers and G. Tchutchulashvili for his help with chemical treatment of Si wafers.

Conflicts of Interest: The authors declare no conflict of interest.

References

1. Ng, H.M.; Cho, A.Y. Investigation of Si doping and impurity incorporation dependence on the polarity of GaN by molecular beam epitaxy. *J. Vac. Sci. Technol. B* **2002**, *20*, 1217–1220. [[CrossRef](#)]
2. Tuomisto, F.; Saarinen, K.; Lucznik, B.; Grzegory, I.; Teisseyre, H.; Suski, T.; Porowski, S.; Hageman, P.R.; Likonen, J. Effect of growth polarity on vacancy defect and impurity incorporation in dislocation-free GaN. *Appl. Phys. Lett.* **2005**, *86*, 031915. [[CrossRef](#)]
3. Li, S.F.; Wang, X.; Fundling, S.; Erenburg, M.; Ledig, J.; Wei, J.D.; Wehmann, H.H.; Waag, A.; Bergbauer, W.; Mandl, M.; et al. Nitrogen-polar core-shell GaN light-emitting diodes grown by selective area metalorganic vapor phase epitaxy. *Appl. Phys. Lett.* **2012**, *101*, 032103. [[CrossRef](#)]
4. Tang, H.; Haffouz, S.; Bardwell, J.A. Si(111) substrates as highly effective pseudomasks for selective growth of GaN material and devices by ammonia-molecular-beam epitaxy. *Appl. Phys. Lett.* **2006**, *88*, 172110. [[CrossRef](#)]
5. Losurdo, M.; Giangregorio, M.M.; Capezzuto, P.; Bruno, G.; Namkoong, G.; Doolittle, W.A.; Brown, A.S. Interplay between GaN polarity and surface reactivity towards atomic hydrogen. *J. Appl. Phys.* **2004**, *95*, 8408–8418. [[CrossRef](#)]
6. Mastro, M.A.; Kryliouk, O.M.; Anderson, T.J.; Davydov, A.; Shapiro, A. Influence of polarity on GaN thermal stability. *J. Cryst. Growth* **2005**, *274*, 38–46. [[CrossRef](#)]
7. Monroy, E.; Sarigiannidou, E.; Fossard, F.; Gogneau, N.; Bellet-Amalric, E.; Rouvière, J.-L.; Monnoye, S.; Mank, H.; Daudin, B. Growth kinetics of N-face polarity GaN by plasma-assisted molecular beam epitaxy. *Appl. Phys. Lett.* **2004**, *84*, 3684–3686. [[CrossRef](#)]
8. Fernández-Garrido, S.; Kong, X.; Gotschke, T.; Calarco, R.; Geelhaar, L.; Trampert, A.; Brandt, O. Spontaneous Nucleation and Growth of GaN Nanowires: The Fundamental Role of Crystal Polarity. *Nano Lett.* **2012**, *12*, 6119–6125. [[CrossRef](#)]
9. Carnevale, S.D.; Kent, T.F.; Phillips, P.J.; Sarwar, A.T.M.G.; Selcu, C.; Klie, R.F.; Myers, R.C. Mixed Polarity in Polarization-Induced p–n Junction Nanowire Light-Emitting Diodes. *Nano Lett.* **2013**, *13*, 3029–3035. [[CrossRef](#)]
10. Ambacher, O.; Smart, J.; Shealy, J.R.; Weimann, N.G.; Chu, K.; Murphy, M.; Schaff, W.J.; Eastman, L.F. Two-dimensional electron gases induced by spontaneous and piezoelectric polarization charges in N- and Ga-face AlGaIn/GaN heterostructures. *J. Appl. Phys.* **1999**, *85*, 3222–3233. [[CrossRef](#)]
11. Alloing, B.; Vézian, S.; Tottereau, O.; Vennéguès, P.; Beraudo, E.; Zúñiga-Pérez, J. On the polarity of GaN micro- and nanowires epitaxially grown on sapphire (0001) and Si(111) substrates by metal organic vapor phase epitaxy and ammoniamolecular beam epitaxy. *Appl. Phys. Lett.* **2011**, *98*, 011914. [[CrossRef](#)]
12. Bertness, K.A.; Memberaaa, S.; Sanford, N.A.; Davydov, A.V. GaN Nanowires Grown by Molecular Beam Epitaxy. *IEEE J. Sel. Top. Quantum Electron.* **2011**, *17*, 847–858. [[CrossRef](#)]

13. Geelhaar, L.; Chèze, C.; Jenichen, B.; Brandt, O.; Pfüller, C.; Münch, S.; Rothmund, R.; Reitzenstein, S.; Forchel, A.; Kehagias, T.; et al. Properties of GaN Nanowires Grown by Molecular Beam Epitaxy. *IEEE J. Sel. Top. Quantum Electron.* **2011**, *17*, 878–888. [[CrossRef](#)]
14. Carnevale, S.D.; Yang, J.; Phillips, P.J.; Mills, M.J.; Myers, R.C. Three-Dimensional GaN/AlN Nanowire Heterostructures by Separating Nucleation and Growth Processes. *Nano Lett.* **2011**, *11*, 866–871. [[CrossRef](#)]
15. Trampert, A.; Ristić, J.; Jahn, U.; Calleja, E.; Ploog, K.H. TEM study of (Ga,Al)N nanocolumns and embedded GaN nanodiscs. *Microsc. Semicond. Mater.* **2003**, *180*, 167–170.
16. Fernández-Garrido, S.; Grandal, J.; Calleja, E.; Sánchez-García, M.A.; López-Romero, D. A growth diagram for plasma-assisted molecular beam epitaxy of GaN nanocolumns on Si(111). *J. Appl. Phys.* **2009**, *106*, 126102. [[CrossRef](#)]
17. Wierzbička, A.; Zytkeiwicz, Z.R.; Kret, S.; Borysiuk, J.; Dłuzewski, P.; Sobanska, M.; Klosek, K.; Reszka, A.; Tchutchulashvili, G.; Cabaj, A.; et al. Influence of substrate nitridation temperature on epitaxial alignment of GaN nanowires to Si(111) substrate. *Nanotechnology* **2013**, *24*, 035703. [[CrossRef](#)]
18. Sobanska, M.; Wierzbička, A.; Klosek, K.; Borysiuk, J.; Tchutchulashvili, G.; Gieraltowska, S.; Zytkeiwicz, Z.R. Arrangement of GaN nanowires grown by plasma-assisted molecular beam epitaxy on silicon substrates with amorphous Al₂O₃ buffers. *J. Cryst. Growth* **2014**, *401*, 657–660. [[CrossRef](#)]
19. Borysiuk, J.; Zytkeiwicz, Z.R.; Sobanska, M.; Wierzbička, A.; Klosek, K.; Korona, K.P.; Perkowska, P.S.; Reszka, A. Growth by molecular beam epitaxy and properties of inclined GaN nanowires on Si(001) substrate. *Nanotechnology* **2014**, *25*, 135610. [[CrossRef](#)] [[PubMed](#)]
20. Concordel, A.; Jacopin, G.; Gayral, B.; Garro, N.; Cros, A.; Rouviere, J.-L.; Daudin, B. Polarity conversion of GaN nanowires grown by plasma-assisted molecular beam epitaxy. *Appl. Phys. Lett.* **2019**, *114*, 172101. [[CrossRef](#)]
21. Zhao, B.; Lockrey, M.N.; Caroff, P.; Wang, N.; Li, L.; Wong-Leung, J.; Tan, H.H.; Jagadish, C. The effect of nitridation on the polarity and optical properties of GaN self-assembled nanorods. *Nanoscale* **2018**, *10*, 11205. [[CrossRef](#)]
22. Hetzl, M.; Kraut, M.; Hoffmann, T.; Stutzmann, M. Polarity Control of Heteroepitaxial GaN Nanowires on Diamond. *Nano Lett.* **2017**, *17*, 3582–3590. [[CrossRef](#)]
23. de Souza Schiaber, Z.; Calabrese, G.; Kong, X.; Trampert, A.; Jenichen, B.; Dias da Silva, J.H.; Geelhaar, L.; Brandt, O.; Fernández-Garrido, S. Polarity-Induced Selective Area Epitaxy of GaN Nanowires. *Nano Lett.* **2017**, *17*, 63–70. [[CrossRef](#)]
24. Green, D.S.; Haus, E.; Wu, F.; Chen, L.; Mishra, U.K.; Speck, J.S. Polarity control during molecular beam epitaxy growth of Mg-doped GaN. *J. Vac. Sci. Technol. B* **2003**, *21*, 1804. [[CrossRef](#)]
25. Pezzagna, S.; Vennegues, P.; Grandjean, N.; Massies, J. Polarity inversion of GaN (0001) by a high Mg doping. *J. Cryst. Growth* **2004**, *269*, 249–256. [[CrossRef](#)]
26. Rosa, A.; Neugebauer, J. Polarity inversion of GaN (0001) surfaces induced by Si adsorption. *Surf. Sci.* **2006**, *600*, 335–339. [[CrossRef](#)]
27. Kong, X.; Li, H.; Albert, S.; Bengoechea-Encabo, A.; Sanchez-Garcia, M.A.; Calleja, E.; Draxl, C.; Trampert, A. Titanium induced polarity inversion in ordered (In,Ga)N/GaN nanocolumns. *Nanotechnology* **2016**, *27*, 065705. [[CrossRef](#)]
28. Mohn, S.; Stolyarchuk, N.; Markurt, T.; Kirste, R.; Hoffmann, M.P.; Collazo, R.; Courville, A.; Di Felice, R.; Sitar, Z.; Vennégues, P.; et al. Polarity Control in Group-III Nitrides beyond Pragmatism. *Phys. Rev. Appl.* **2016**, *5*, 054004. [[CrossRef](#)]
29. Roshko, A.; Brubaker, M.; Blanchard, P.; Harvey, T.; Bertness, K. The role of Si in GaN/AlN/Si(111) plasma assisted molecular beam epitaxy: Polarity and inversion. *Jpn. J. Appl. Phys.* **2019**, *58*, SC1050. [[CrossRef](#)]
30. Roshko, A.; Brubaker, M.D.; Blanchard, P.T.; Harvey, T.E.; Bertness, K.A. Eutectic Formation, V/III Ratio, and Controlled Polarity Inversion in Nitrides on Silicon. *Phys. Status Solidi B* **2020**, *257*, 1900611. [[CrossRef](#)]
31. Zúñiga-Pérez, J.; Consonni, V.; Lymperakis, L.; Kong, X.; Trampert, A.; Fernández-Garrido, S.; Brandt, O.; Renevier, H.; Keller, S.; Hestroffer, K.; et al. Polarity in GaN and ZnO: Theory, measurement, growth, and devices. *Appl. Phys. Rev.* **2016**, *3*, 041303. [[CrossRef](#)]
32. Minj, A.; Cros, A.; Garro, N.; Colchero, J.; Auzelle, T.; Daudin, B. Assessment of Polarity in GaN Self-Assembled Nanowires by Electrical Force Microscopy. *Nano Lett.* **2015**, *15*, 6770–6776. [[CrossRef](#)]

33. Sobanska, M.; Klosek, K.; Borysiuk, J.; Kret, S.; Tchutchulasvili, G.; Gieraltowska, S.; Zytkeiwicz, Z.R. Enhanced catalyst-free nucleation of GaN nanowires on amorphous Al₂O₃ by plasma-assisted molecular beam epitaxy. *J. Appl. Phys.* **2014**, *115*, 043517. [[CrossRef](#)]
34. Sobanska, M.; Korona, K.P.; Zytkeiwicz, Z.R.; Klosek, K.; Tchutchulashvili, G. Kinetics of self-induced nucleation and optical properties of GaN nanowires grown by plasma-assisted molecular beam epitaxy on amorphous Al_xO_y. *J. Appl. Phys.* **2015**, *118*, 184303. [[CrossRef](#)]
35. Klosek, K.; Sobanska, M.; Tchutchulashvili, G.; Zytkeiwicz, Z.R.; Teisseyre, H.; Klopotowski, L. Optimization of nitrogen plasma source parameters by measurements of emitted light intensity for growth of GaN by molecular beam epitaxy. *Thin Solid Films* **2013**, *534*, 107–110. [[CrossRef](#)]
36. Ino, S. Some New Techniques in Reflection High Energy Electron Diffraction (RHEED) Application to Surface Structure Studies. *Jpn. J. Appl. Phys.* **1977**, *16*, 891–908. [[CrossRef](#)]
37. Osakabe, N.; Yagi, K.; Honjo, G. Reflection Electron Microscope Observations of Dislocations and Surface Structure Phase Transition on Clean (111) Silicon Surfaces. *Jpn. J. Appl. Phys.* **1980**, *19*, L309–L312. [[CrossRef](#)]
38. Cheze, C.; Geelhaar, L.; Trampert, A.; Riechert, H. In situ investigation of self-induced GaN nanowire nucleation on Si. *Appl. Phys. Lett.* **2010**, *97*, 043101. [[CrossRef](#)]
39. Consonni, V.; Hanke, M.; Knelangen, M.; Geelhaar, L.; Trampert, A.; Riechert, H. Nucleation mechanisms of self-induced GaN nanowires grown on an amorphous interlayer. *Phys. Rev. B* **2011**, *83*, 035310. [[CrossRef](#)]
40. Fernández-Garrido, S.; Zettler, J.K.; Geelhaar, L.; Brandt, O. Monitoring the Formation of Nanowires by Line-of-Sight Quadrupole Mass Spectrometry: A Comprehensive Description of the Temporal Evolution of GaN Nanowire Ensembles. *Nano Lett.* **2015**, *15*, 1930–1937. [[CrossRef](#)]
41. Sobanska, M.; Fernández-Garrido, S.; Zytkeiwicz, Z.R.; Tchutchulashvili, G.; Gieraltowska, S.; Brandt, O.; Geelhaar, L. Self-assembled growth of GaN nanowires on amorphous Al_xO_y: From nucleation to the formation of dense nanowire ensembles. *Nanotechnology* **2016**, *27*, 325601. [[CrossRef](#)]
42. Gieraltowska, S.; Wachnicki, L.; Witkowski, B.S.; Mroczynski, R.; Dluzewski, P.; Godlewski, M. Characterization of dielectric layers grown at low temperature by atomic layer deposition. *Thin Solid Films* **2015**, *577*, 97–102. [[CrossRef](#)]
43. Colchero, J.; Gil, A.; Baró, A.M. Resolution enhancement and improved data interpretation in electrostatic force microscopy. *Phys. Rev. B* **2001**, *64*, 245403. [[CrossRef](#)]
44. Palacios-Lidón, E.; Abellán, J.; Colchero, J.; Munuera, C.; Ocal, C. Quantitative electrostatic force microscopy on heterogeneous nanoscale samples. *Appl. Phys. Lett.* **2005**, *87*, 154106. [[CrossRef](#)]
45. Rodriguez, B.J.; Yang, W.-C.; Nemanich, R.J.; Gruverman, A. Scanning probe investigation of surface charge and surface potential of GaN-based heterostructures. *Appl. Phys. Lett.* **2005**, *86*, 112115. [[CrossRef](#)]
46. Hestroffer, K.; Leclere, C.; Bougerol, C.; Renevier, H.; Daudin, B. Polarity of GaN nanowires grown by plasma-assisted molecular beam epitaxy on Si(111). *Phys. Rev. B* **2011**, *84*, 245302. [[CrossRef](#)]
47. Hestroffer, K.; Daudin, B. A RHEED investigation of self-assembled GaN nanowire nucleation dynamics on bare Si and on Si covered with a thin AlN buffer layer. *Phys. Status Solidi RRL* **2013**, *7*, 835–839. [[CrossRef](#)]
48. Largeau, L.; Dheeraj, D.L.; Tchernycheva, M.; Cirlin, G.E.; Harmand, J.C. Facet and in-plane crystallographic orientations of GaN nanowires grown on Si(111). *Nanotechnology* **2008**, *19*, 155704. [[CrossRef](#)]
49. Furtmayr, F.; Vielemeyer, M.; Stutzmann, M.; Arbiol, J.; Estradé, S.; Peirò, F.; Morante, J.R.; Eickhoff, M. Nucleation and growth of GaN nanorods on Si(111) surfaces by plasma-assisted molecular beam epitaxy—The influence of Si- and Mg-doping. *J. Appl. Phys.* **2008**, *104*, 034309. [[CrossRef](#)]
50. Furtmayr, F.; Vielemeyer, M.; Stutzmann, M.; Laufer, A.; Meyer, B.K.; Eickhoff, M. Optical properties of Si- and Mg-doped gallium nitride nanowires grown by plasma-assisted molecular beam epitaxy. *J. Appl. Phys.* **2008**, *104*, 074309. [[CrossRef](#)]
51. Morita, Y.; Miki, K.; Tokumoto, H. Atomic Structure of Hydrogen-Terminated Si(111) Surfaces by Hydrofluoric Acid Treatments. *Jpn. J. Appl. Phys.* **1991**, *30*, 3570–3574. [[CrossRef](#)]
52. Thornton, J.M.C.; Williams, R.H. A photoemission study of passivated silicon surfaces produced by etching in solutions of HF. *Semicond. Sci. Technol.* **1989**, *4*, 847. [[CrossRef](#)]
53. Takahagi, T.; Nagai, I.; Ishitani, A.; Kuroda, H.; Nagasawa, Y. The formation of hydrogen passivated silicon single-crystal surfaces using ultraviolet cleaning and HF etching. *J. Appl. Phys.* **1988**, *64*, 3516. [[CrossRef](#)]
54. Thornton, J.M.C.; Williams, R.H. An S/XPS study of hydrogen terminated, ordered silicon (100) and (111) surfaces prepared by chemical etching. *Phys. Scr.* **1990**, *41*, 1047. [[CrossRef](#)]

55. Miki, K.; Sakamoto, K.; Sakamoto, T. Surface preparation of Si substrates for epitaxial growth. *Surf. Sci.* **1998**, *406*, 312–327. [[CrossRef](#)]
56. Wierzbicka, A.; Tchutchulashvili, G.; Sobanska, M.; Klosek, K.; Minikayev, R.; Domagala, J.Z.; Borysiuk, J.; Zytkeiwicz, Z.R. Arrangement of GaN nanowires on Si(001) substrates studied by X-ray diffraction: Importance of silicon nitride interlayer. *Appl. Surf. Sci.* **2017**, *425*, 1014–1019. [[CrossRef](#)]
57. Wright, S.; Kroemer, H. Reduction of oxides on silicon by heating in a gallium molecular beam at 800 °C. *Appl. Phys. Lett.* **1980**, *36*, 210. [[CrossRef](#)]
58. Chin, C.W.; Yam, F.K.; Beh, K.P.; Hassan, Z.; Ahmad, M.A.; Yusof, Y.; Mohd Bakhori, S.K. The growth of heavily Mg-doped GaN thin film on Si substrate by molecular beam epitaxy. *Thin Solid Films* **2011**, *520*, 756–760. [[CrossRef](#)]
59. Limbach, F.; Caterino, R.; Gotschke, T.; Stoica, T.; Calarco, R.; Geelhaar, L.; Riechert, H. The influence of Mg doping on the nucleation of self-induced GaN nanowires. *AIP Adv.* **2012**, *2*, 012157. [[CrossRef](#)]
60. Husseini, A.S.; Thahab, S.M.; Hassan, Z.; Chin, C.W.; Abu Hassan, H.; Ng, S.S. High Al-content Al_xGa_{1-x}N epilayers grown on Si substrate by plasma-assisted molecular beam epitaxy. *J. Alloys Compd.* **2009**, *487*, 24–27. [[CrossRef](#)]
61. Lee, J.H.; Wang, Z.M.; Salamo, G.J. Ga-triggered oxide desorption from GaAs (100) and non-(100) substrates. *Appl. Phys. Lett.* **2006**, *88*, 252108. [[CrossRef](#)]
62. Wasilewski, Z.R.; Baribeau, J.-M.; Beaulieu, M.; Wu, X.; Sproule, G.I. Studies of oxide desorption from GaAs substrates via Ga₂O₃ to Ga₂O conversion by exposure to Ga flux. *J. Vac. Sci. Technol. B* **2004**, *22*, 1534. [[CrossRef](#)]
63. Kern, W.; Puotinen, D.A. Cleaning solutions based on hydrogen peroxide for use in silicon semiconductor technology. *RCA Rev.* **1970**, *31*, 187–206.
64. Ishizaka, A.; Shiraki, Y. Low Temperature Surface Cleaning of Silicon and Its Application to Silicon MBE. *J. Electrochem. Soc.* **1986**, *133*, 666. [[CrossRef](#)]
65. Eftychis, S.; Kruse, J.; Koukoula, T.; Kehagias, T.; Komninou, P.; Adikimenakis, A.; Tsagaraki, K.; Androulidaki, M.; Tzanetakis, P.; Iliopoulos, E.; et al. Understanding the effects of Si(111) nitridation on the spontaneous growth and properties of GaN nanowires. *J. Cryst. Growth* **2016**, *442*, 8–13. [[CrossRef](#)]
66. Calleja, E.; Sánchez-García, M.A.; Sánchez, F.J.; Calle, F.; Naranjo, F.B.; Muñoz, E.; Molina, S.I.; Sánchez, A.M.; Pacheco, F.J.; García, R. Growth of III-nitrides on Si(111) by molecular beam epitaxy Doping, optical, and electrical properties. *J. Cryst. Growth* **1999**, *201/202*, 296–317. [[CrossRef](#)]
67. Mohd Yusoff, M.Z.; Hassan, Z.; Chin, C.W.; Abu Hassan, H.; Abdullah, M.J.; Ahmad, M.A.; Yusof, Y. Fabrication of GaN homo-junction on Si(111) substrate for sensor applications. *J. Mol. Eng. Mater.* **2013**, *1*, 1250006. [[CrossRef](#)]
68. Kern, W. The Evolution of Silicon Wafer Cleaning Technology. *J. Electrochem. Soc.* **1990**, *137*, 1887. [[CrossRef](#)]
69. Sobanska, M.; Zytkeiwicz, Z.R.; Klosek, K.; Kruszka, R.; Golaszewska, K.; Ekielski, M.; Gieraltowska, S. Selective area formation of GaN nanowires on GaN substrates by the use of amorphous Al_xO_y nucleation layer. *Nanotechnology* **2020**, *31*, 184001. [[CrossRef](#)]
70. Sobanska, M.; Zytkeiwicz, Z.R.; Ekielski, M.; Klosek, K.; Sokolovskii, A.S.; Dubrovskii, V.G. Surface Diffusion of Gallium as the Origin of Inhomogeneity in Selective Area Growth of GaN Nanowires on Al_xO_y Nucleation Stripes. *Cryst. Growth Des.* **2020**, *20*, 4770–4778. [[CrossRef](#)]
71. Sobanska, M.; Zytkeiwicz, Z.R.; Calabrese, G.; Geelhaar, L.; Fernández-Garrido, S. Comprehensive analysis of the self-assembled formation of GaN nanowires on amorphous Al_xO_y: In situ quadrupole mass spectrometry studies. *Nanotechnology* **2019**, *30*, 154002. [[CrossRef](#)] [[PubMed](#)]
72. Sobanska, M.; Dubrovskii, V.G.; Tchutchulashvili, G.; Klosek, K.; Zytkeiwicz, Z.R. Analysis of Incubation Times for the Self-Induced Formation of GaN Nanowires: Influence of the Substrate on the Nucleation Mechanism. *Cryst. Growth Des.* **2016**, *16*, 7205–7211. [[CrossRef](#)]

73. Corfdir, P.; Hauswald, C.; Zettler, J.K.; Flissikowski, T.; Lähnemann, J.; Fernández-Garrido, S.; Geelhaar, L.; Grahn, H.T.; Brandt, O. Stacking faults as quantum wells in nanowires: Density of states, oscillator strength, and radiative efficiency. *Phys. Rev. B* **2014**, *90*, 195309. [[CrossRef](#)]

Publisher's Note: MDPI stays neutral with regard to jurisdictional claims in published maps and institutional affiliations.



© 2020 by the authors. Licensee MDPI, Basel, Switzerland. This article is an open access article distributed under the terms and conditions of the Creative Commons Attribution (CC BY) license (<http://creativecommons.org/licenses/by/4.0/>).